EVALUATING THE IMPACT OF LULC CHANGES ON FLASH FLOOD USING HEC-HMS: A CASE STUDY FOR SYLHET REGION

Faishal Ahmed*[1], Md. Abresham Ibne Wahid[2], Musabbir Turjo[3], Md Azmain Rahman[4], Tamjidul Islam Illin[5] and A.K.M. Rashnat Hossain[6]

[1] *Department of Water Resources Engineering, Bangladesh University of Engineering and Technology, Dhaka-1000, Bangladesh, e-mail: faishalahmed413@gmail.com*
[2] *Department of Water Resources Engineering, Bangladesh University of Engineering and Technology, Dhaka-1000, Bangladesh, e-mail: abresham4896@gmail.com*
[3] *Department of Water Resources Engineering, Bangladesh University of Engineering and Technology, Dhaka-1000, Bangladesh, e-mail: musabbir.tj99@gmail.com*
[4] *Department of Water Resources Engineering, Bangladesh University of Engineering and Technology, Dhaka-1000, Bangladesh, e-mail: md.azmainr@gmail.com*
[5] *Department of Water Resources Engineering, Bangladesh University of Engineering and Technology, Dhaka-1000, Bangladesh, e-mail: 1816018@wre.buet.ac.bd*
[6] *Department of Water Resources Engineering, Bangladesh University of Engineering and Technology, Dhaka-1000, Bangladesh, e-mail: 1816013@wre.buet.ac.bd*

***Corresponding Author**

ABSTRACT

Evaluating the impact of alterations in land use and land cover (LULC) on watershed hydrological responses is of paramount importance for implementing effective flood-control measures. In recent times, the Sylhet region has experienced a surge in flash floods, leading to substantial economic losses and the displacement of millions of residents. The primary driver behind these unexpected floods has been intense rainfall in the upstream area, particularly in Meghalaya. However, recent research has uncovered a connection between canopy density and runoff in the downstream region. The LULC patterns in both the Sylhet area and its upstream regions have been evolving in parallel with global trends. Notably, since 1991, the Meghalaya region has witnessed an alarming 18% reduction in canopy cover due to hill cutting for agricultural and human activities. This study has developed a Hydrologic Engineering Center Hydrologic Model System (HEC-HMS) tailored to the Sylhet region. The land use and land cover in the basin were assessed, and the curve number and imperviousness were determined. These values were incorporated into the model for calibration (2004) and validation (2009). Then the validated model was used to simulate the flash floods of specific years in that region. Subsequently, the lag time between the peak rainfall in Meghalaya and the occurrence of flooding above the danger level in the Sylhet region was analyzed. The study revealed that in 2002, the developed area comprised 2.71% of the landscape, while dense forest covered 35.47%. However, by 2022, these figures shifted significantly, with developed areas expanding to 10.63% and dense forests diminishing to 23.39%. As a result of the land use and land cover changes, the time it takes for a flood to occur after rainfall events has decreased, shifting from 12 hours in 2002 to 7 hours in 2022. Our study underscores the intricate relationship between changing LULC patterns and the occurrence of flash floods, primarily attributed to increased impervious surfaces resulting from urban development and reduced forest cover. As the developed area expands and dense forests dwindle, the onset of flash floods has accelerated. Understanding the evolving land use trends and their impact on flash flood timing is essential for implementing proactive measures to address the increasing risks linked to rapid urban development in the study region.

Keywords: *Flash-Flood, LULC, HEC-HMS, Lag Time, Imperviousness*

1. INTRODUCTION

Flash floods are defined as floods that arrive quickly, leaving just a short period for warnings to be prepared. (Kementerian, 2018). Extreme precipitation, the breakdown of man-made infrastructure such as dams, or complicated water-snow interactions are all viable reasons to produce flash floods. When compared to riverine floods, the rapid development of flash floods provides extra obstacles for early prediction and risk protection measures (Zanchetta & Coulibaly, 2020). The system for reducing casualties from many natural disasters has shown consistent improvement, but the comparable system for flash floods, which can strike suddenly and bring additional hazards like landslides, mudflows, infrastructure damage, and fatalities, has not progressed as effectively. This results in flash floods being the deadliest convective storm-related event annually (Kementerian, 2018; Severe, 1996). This discrepancy highlights the critical need for improved planning and mitigation methods targeted especially to flash flood occurrences (Severe, 1996).

Bangladesh, along with the Indian state of West Bengal, is located in the lowest section of the Hindu Kush - Himalayan Region (HKH) and is known as one of the world's most flood-prone countries (WMO & GWPS, 2003). Geographically, Bangladesh is located between the Himalayas in the north and the Bay of Bengal in the south. Most parts of Bangladesh are floodplain areas with numerous rivers (Rashid et al., 2015). Although the Ganges–Brahmaputra–Meghna Delta (GBM Delta) covers only 7% of the total area within the country, an estimated discharge of 93% flows over the territories of Bangladesh toward the Bay of Bengal. This discharge is the prime factor behind hydrological disasters in Bangladesh (Islam, 2016). Flash floods have been recorded in Bangladesh since the 1980s (BWDB 2015). In recent years, flash floods have become a serious concern for the lives and livelihoods of the people in Bangladesh (Shuvo et al., 2021). These sudden flood activities have a serious impact on the agriculture of Bangladesh (Alamgir et al., 2020; M. Rashid & Yasmeen, 2018). In Bangladesh, the main cause of flash floods is rainfall (Das et al., 2017). The need to forecast floods in Bangladesh has been growing since the 1970s, and more so in recent decades (Adnan & Bhuiyan, 2010); such forecasts should reduce the livelihood vulnerability of the people and maintain sustainable economic growth in the country. However, forecasting flash flood events has been very challenging, mostly because of their unpredictable nature (Jain et al., 2018).

Lead time and lag time are two very important parameters for the prediction of flash floods (L. et al., 2001; Wu et al., 2019). In addition, lag time is highly important for understanding the characteristics of flood events and their associated features (for example—accumulation of rainfall, duration of rainfall, topography of the basin, river network, and other factors), since the chances of having identical lag times for the two flash flood events are very small (Qi et al., 2021).Thus, the calculation of lag time from hydrographs has been given priority in this research. Again, there are challenges in model-based calculations for flood forecasting (Chen et al., 2020). Therefore, they were also considered when analyzing the results of this research.

(Mandal & Chakrabarty, 2016) studied over upper teesta basin, India in which geospatial input for CN grid data, incorporating land use, hydrological soil group, and eluviation, informed a hydraulic model (HEC-RAS, HEC-HMS) were used to assess the flash flood probability. The simulation, validated against the 1968 flood event, demonstrated 78% accuracy in reflecting the actual flooded area, affirming the model's effectiveness. (El Alfy, 2016) studied over Jazan region, Saudi Arabia and indicates that swift urbanization has detrimental effects on hydrological processes, notably by expanding onto significant alluvial channels. This diminishes infiltration into the underlying alluvium, elevating runoff, and causing increased flood peaks and volumes even with brief, low-intensity rainfall. (Janicka & Kanclerz, 2023) studied over Wirynka catchment, Poland and the investigation revealed that rapid urbanization negatively impacts hydrological processes, leading to diminished infiltration capacity and heightened water runoff. This elevates the vulnerability to flooding and waterlogging, emphasizing the critical need for effective rainwater management in the region. Examining Hyderabad city, India, (Singh, 2018) revealed that urbanization disturbs the natural water balance, amplifying impervious areas and decreasing infiltration. Consequently, urban catchments

experience escalated runoff, resulting in elevated flood peaks, even with short-duration, low-intensity rainfall.

However, the majority of studies concentrate on regions beyond the Sylhet region, often overlooking the specific flash flood events in this area. Therefore, this study aims to develop a HEC HMS model to analyze flash floods in the Sylhet region. Additionally, it seeks to examine the lag time of flash floods in the Sylhet region from 2002 to 2022, considering the impact of land use and land cover (LULC) changes in various flood occurrences.

2. METHODOLOGY

2.1 Study area

The study area was selected to be the Sylhet region of Bangladesh, which resides in the northwestern part of our country. The upstream of water inflow comes from the Meghalaya state of India and the outlet was selected to be Sunamganj station (SW-269). It has been observed that after watershed delineation, almost half of the basin is situated in Bangladesh and other half in India. The Figure 1. Shows the details of study area.

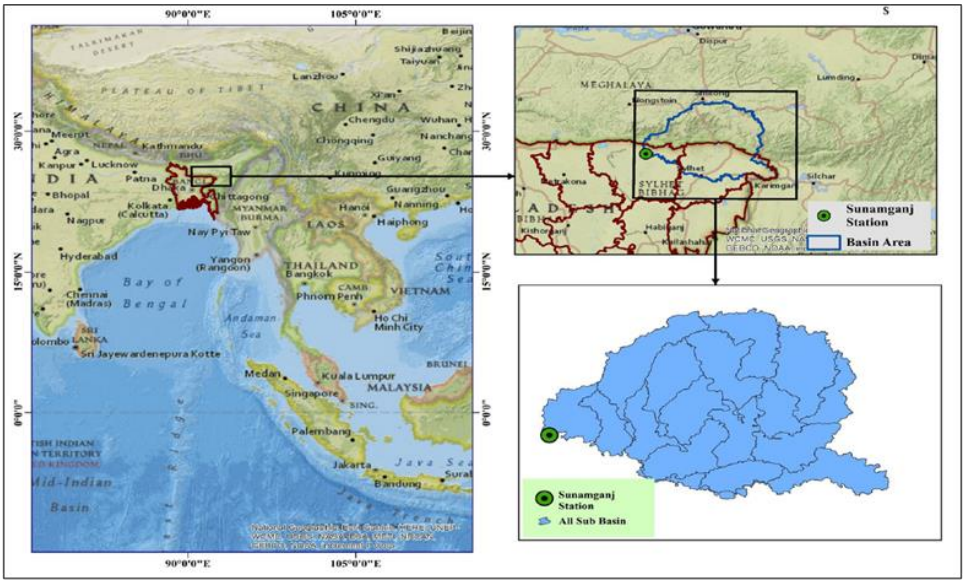

Figure 1. Study Area

2.2 Data Collection

The various data required for flash flood simulation included: Digital Elevation Model of the study area, reflectance data for 7 bands in order to create the LULC maps, hourly Copernicus precipitation dataset from ERA 5 website, & discharge & water level data from Bangladesh Water Development Board for the outlet station SW-269. DEMs play a pivotal role in fully distributed hydraulic and hydrological models by extracting essential information like lateral multiple flow paths, water accumulation and dispersion, and delineation of catchment boundaries (Vaze et al., 2010). Findings from various studies indicate that the Copernicus DEM exhibits higher accuracy than the SRTM, with Cop-DEM demonstrating better RMSE and MAE by 6%-44% and 5%-53%, respectively, particularly in urban and mountainous regions (Ghannadi et al., 2023). The years for which data was collected and their spatial resolution are shown in the Table 1. The Copernicus program of Europe uses precise and timely data from satellites and other sources to offer crucial information services to enhance the management of the environment. The accuracy of the satellite precipitation data is excellent generally, although there is a minor overestimation (Feidas, 2010).

Data	Source	Period	Resolution
DEM	Copernicus	2022	30m x 30m
Satellite Image	USGS Earth Explorer	2002, 2004, 2009, 2011, 2017, 2022	30m x 30m
Hourly Precipitation	Copernicus	2002, 2004, 2009, 2011, 2017, 2022	0.25° x 0.25°
Monthly Discharge	BWDB (SW 269)	2004, 2009	Gauged
Daily Water Level	BWDB (SW 269)	2002, 2004, 2009, 2011, 2017, 2022	Gauged

Table 1. Data source

2.3 Watershed Delineation

The DEM file for all of Bangladesh was downloaded from FABDEM (Forest and Buildings removed Copernicus DEM). FABDEM, a groundbreaking universal Digital Elevation Model (DEM) at 30-meter resolution, effectively eliminates buildings and forests. Employing a correction algorithm, it rectifies biases in the Copernicus GLO 30 DSM caused by surface objects, enhancing datasets for universal modeling of natural hazardous events (Saberi et al., 2023). Then it was preprocessed in ArcGIS. A rectangular portion of the DEM file was clipped containing the Meghalaya & Sylhet regions which was then imported to HEC-HMS for watershed delineation. In running the operation 'Identify Streams', an area of 100 km^2 was used, and the SW-269 station latitude-longitude was used to import a point shape file as the outlet. The resulting sub-basins were then merged so that their areas were more or less the same. After merging, a total of 16 sub-basins & 13 reaches were obtained as shown in Figure 2.

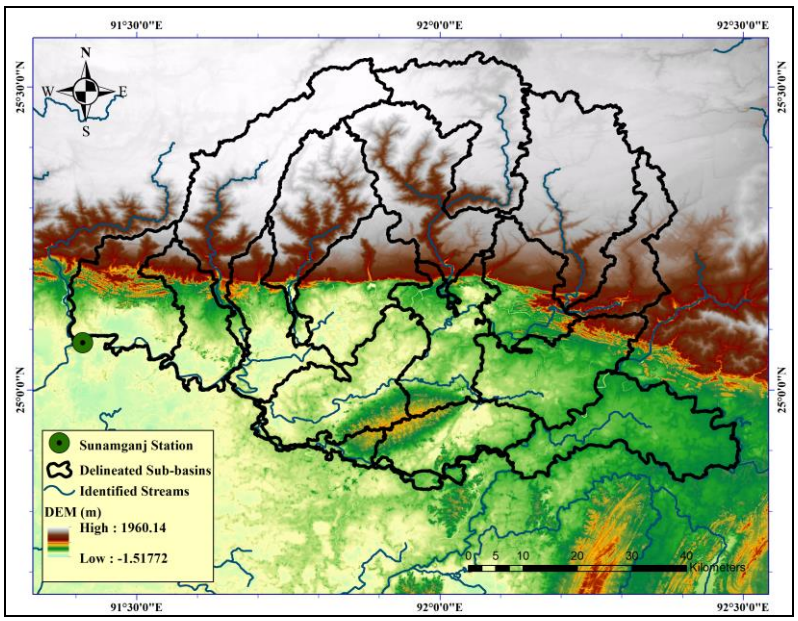

Figure 2. Watershed Delineation

2.4 Procedure of LULC map preparation:

First, Surface reflectance bands (B1-B7) of Landsat 8-9 OLI Collection-2 Level-1 was downloaded from USGS earthexplo0rer. Then, separate 7 images of the 7 bands were imported in ArcGIS and merged into a single composite raster. The study area was then clipped from the raster using shapefile. Then, the clipped raster was classified into 40 categories using 'Iso-Cluster Unsupervised Classification' algorithm of ArcGIS (Nijhawan et al., 2017). After that, with the help of Google Earth

and local topography baseman, the 40 classes were manually reclassified into six distinct categories Open Water, Developed Area, Barren Land, Grass Land, Forest and Cultivated Land. Figure 3. shows the LULC map of 2022 that was produced for the study area. The basin shapefile consisting of each subbasin as a polygon feature was imported and projected. Finally, Using the 'zonal' tool of ArcGIS, every land use type area for every feature i.e., subbasin was calculated and tabulated. The table was later used for Curve Number and Imperviousness calculation.

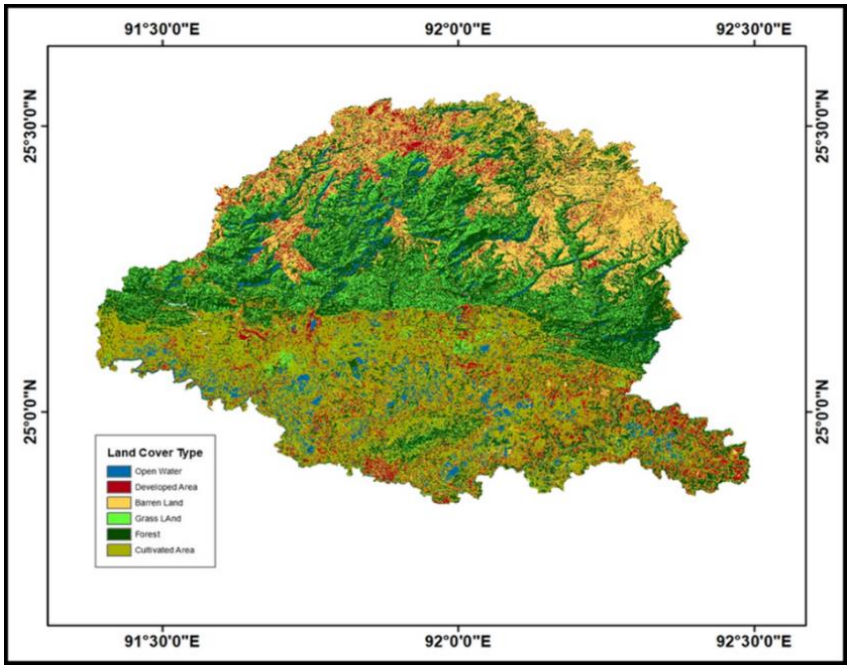

Figure 3. Land Use Land Cover Map

2.5 Calculation of Curve Number and Imperviousness for Subbasins:

From the HEC-HMS Technical Reference Manual, Curve Number and Percent Imperviousness value for each land use type was obtained, shown in Table 2. From the tabulated land use-wise subbasin area, the weighted average of Curve Number (CN) was calculated meaning, each land use type area in a subbasin was multiplied by the respective curve number and then divided by total area of that subbasin which yielded the CN value representative of the sub-basin area. By the exactly same procedure, Percent Imperviousness value was calculated for each subbasins.

Land Class	Curve Number	Imperviousness
Open Water	98	100
Developed Area	81	80
Barren Land	91	20
Grass land	79	20
Forest	70	10
Cultivated Area	85	20

Table 2. Curve number and Imperviousness

From the LULC histogram plot, it is evident that the canopy cover is decreasing while the developed area is increasing over the years in our study area. Which consequently is causing steady increase in imperviousness in the subbasin which is noticeable in percent imperviousness plot over the years.
As the imperviousness is consistently increasing, there the runoff is accumulating faster which means the lag time between the rainfall and the peak flood is consistently decreasing. In other words, the flash flood is occurring much sooner in the recent years than before. Curve number and

Imperviousness are defined as Equations (1) and (2), respectively (HEC-HMS Technical Reference Manual).

$$CNcomposite = \frac{\Sigma Ai * CNi}{\Sigma Ai} \quad \text{.....(1)}$$

Where:
- $CN_{composite}$ is the composite curve number for the sub-basins.
- A_i is the area of the i-th land use.
- CN_i is the curve number for the i-th land use.

$$Imcomposite = \frac{\Sigma Ai * Imi}{\Sigma Ai} \quad \text{.....(2)}$$

Where:
- $Im_{composite}$ is the composite imperviousness for the sub-basins.
- A_i is the area of the i-th land use or cover category.
- Im_i is the imperviousness value for the i-th land use or cover category.

2.6 Preparation of Rating Curve:

Only quarterly discharge data were available from BWDB but daily discharge was required to run the model. For this, rating curves were created for the calibration (2004) & validation (2009) years. The rating curve has the equation of the form $Q = CW^n$, where Q is the discharge, C & n are constants & W is the water depth. Taking logarithm on both sides and applying linear regression, the constants C & n were calculated, which were then used to calculate daily discharge by using daily water level data. Figure 4. illustrates an example rating curve that was developed for the year 2004. The danger water level at which flood occurs at Sunamganj station according to Flood Forecasting & Warning Centre, BWDB is 7.8 mMSL. The rating curves were used for finding the flood level discharges corresponding to this water level, & the values were around 1950 m^3/s for 2004 & 2100 m^3/s for 2009. A discharge of 2000 m^3/s was used in this study as the discharge at which flood occurs. This discharge was later used to identify the time lag between rainfall peak and flood arrival.

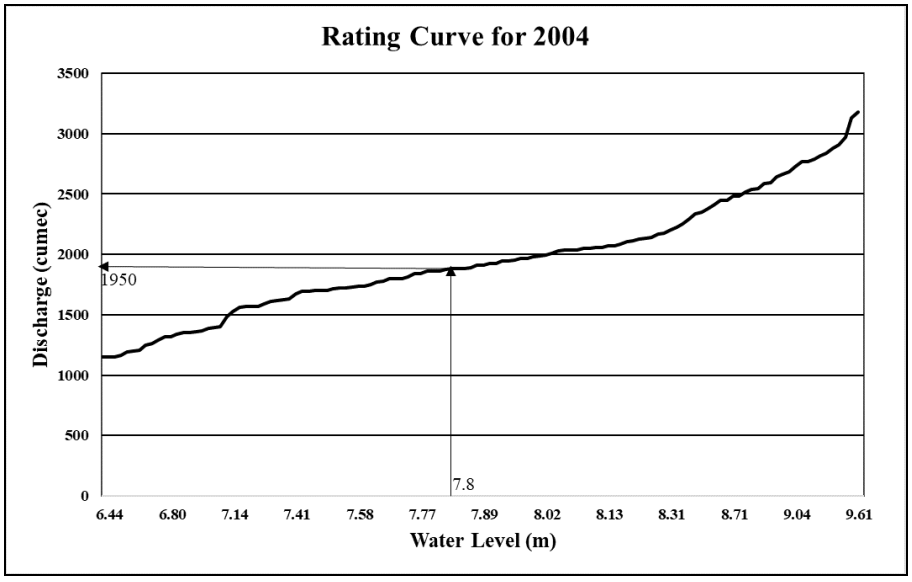

Figure 4. Rating Curve

2.7 Model Setup:

The basin model in HEC-HMS was setup by applying the following methods:
Canopy Method: Simple Canopy Method

Surface Method: Simple Surface Method
Loss Method: SCS Curve Number
Transform Method: SCS Unit Hydrograph
Baseflow method: Recession Method
Routing Method: Muskingum

The CN and Imperviousness obtained from the LULC maps were inputted as parameters of the SCS Curve Number method. Then random initial values were assigned to other parameters. Then the meteorological model was setup by creating 16 precipitation gages for the 16 sub-basins using the data extracted from ERA 5 applying Python coding. A discharge gage containing the observed discharges (for calibration & validation years) obtained from the rating curve was also assigned to the outlet. The model was run for the months of June to September (monsoon) for the years 2002, 2004, 2009, 2011, 2017, 2022. The years 2004 & 2009 were chosen as the calibration and validation year respectively.

2.8 Model Calibration & Validation:

After the model was setup, it was run and calibrated for the year 2004. There were a lot of calibrating parameters for our HEC-HMS model, & both manual calibrations along with HEC-HMS optimization trials were utilized. Some of the parameters were unable to converge using optimization trials, which were also calibrated manually. The manually calibrated parameters were initial storage & max storage for both simple canopy and simple surface methods, Muskingum K and X of routing method, & the initial discharge & recession constant for baseflow recession method. The other parameters, namely lag time (SCS Unit Hydrograph method) & Ratio to Peak (recession method) were optimized automatically using trials. The calibrated discharge and observed discharge are shown in calibration curve (Figure 5). The CN and imperviousness of the sub-basins were obtained from the 2009 LULC map. The calibrated parameters were then used to validate the model for the dataset of 2009 and produce the validation curve (Figure 6). Table 3. shows the parameters that were obtained as a measure of the accuracy of the calibrated and validated model:

Parameter	Value for Calibration	Value after Validation
RMSE	0.4	0.55
Nash Sutcliffe	0.789	0.791
Percent Bias	1.61	1.75
Correlation Coefficient	0.9245	0.892

Table 3. Statistical Parameters for Calibration and Validation

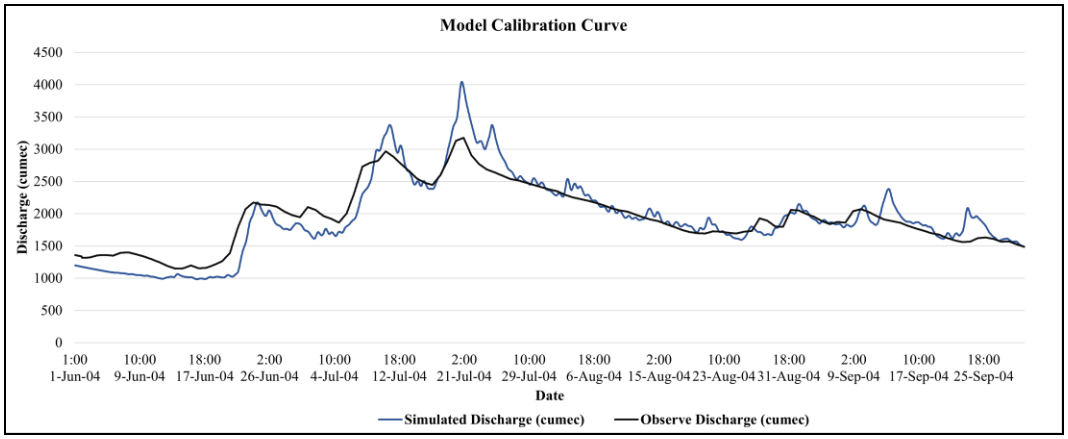

Figure 5. Calibration curve

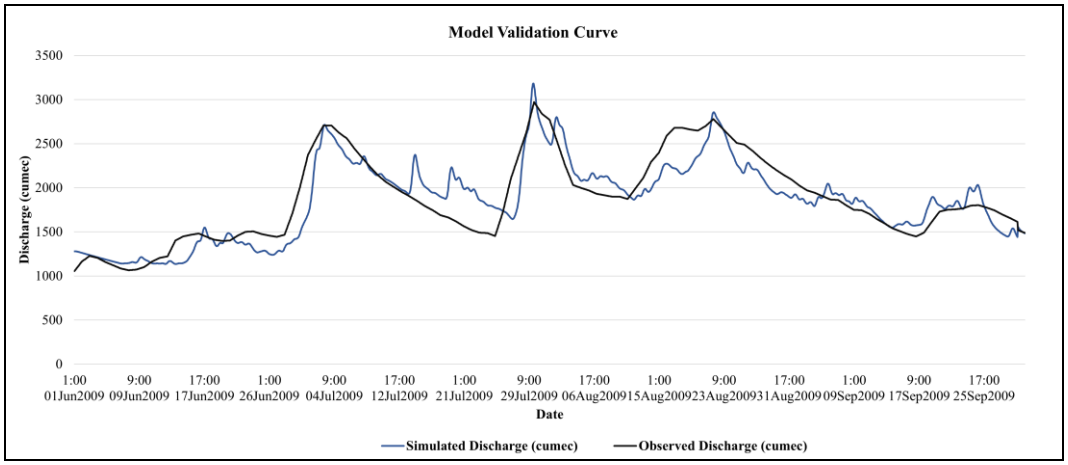

Figure 6. Validation curve

The accuracy parameters of our calibration and validation model produced the numbers below which given the circumstances show a good simulated discharge for our outlet. According to (Arnold et al., 2015) for a daily, monthly or annual hydrological analysis (discharge or flow) the Table 4 can be applied for Nash Sutcliffe Efficiency (NSE) as an evaluation criterion:

Unsatisfactory	Satisfactory	Very Good	Good
NSE =< 0.50	0.50 < NSE =< 0.70	0.70 < NSE =< 0.80	NSE > 0.80

Table 4. Acceptable Value Range of NSE

Table 5 shows the acceptable Percent Bias (P-Bias) values (P Fernandes et al., 2023):

Very good performance	Good Performance
<10%	10%-15%

Table 5. Acceptable Value Range of P-Bias

3. RESULT AND DISCUSSION

Through analyzing the LULC changes, it was observed that the percentage of canopy was decreasing as the years progressed (Figure 7). It started with 35.48 percent and finally came to 23.39 percent, where a significant reduction happened between 2002-2004. But it can also be seen that developed area showed an increasing trend (Figure 7). From 2.31 percent in 2002 to 10.63 percent in 2022. This shows that due to industrial rapid advancement the necessity for developed area is increasing day by day and the price is being paid by forest areas.

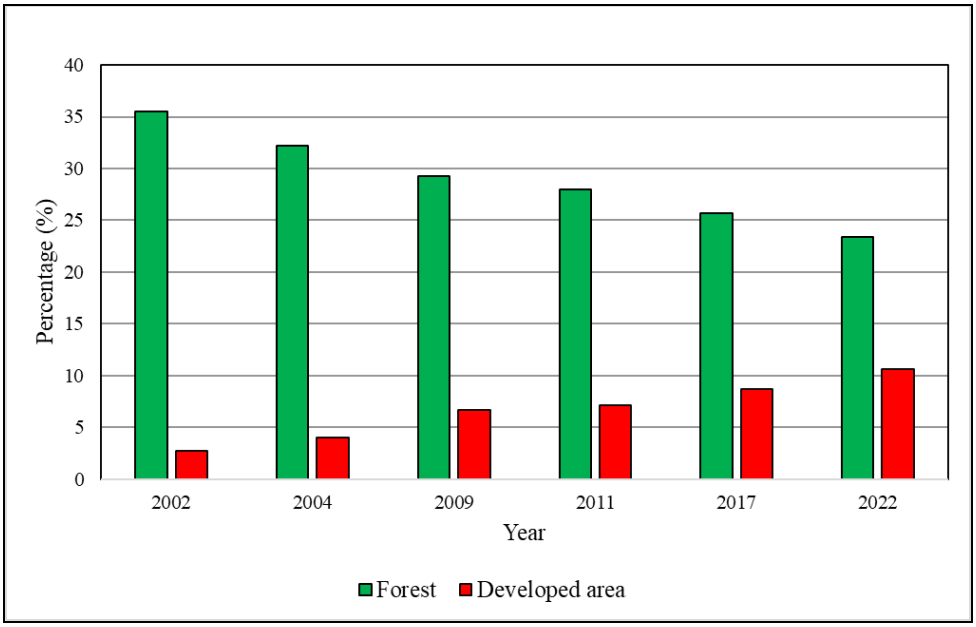

Figure 7. Change of canopy and developed area

Urbanization and conventional development practices contribute to heightened surfaces imperviousness, leading to elevated surface runoff, accelerated runoff velocity, reduced time of concentration, and diminished water quality (Dietz, 2007). The rise in impervious surfaces is directly linked to the expanding developed areas within the study region, primarily driven by the growth of urban areas (Figure 7).

We obtained the time interval between rainfall in the Meghalaya region and flood in the Sylhet-Sunamganj area from the simulation. For this, the average rainfall of the sub-basins whose majority area falls within Meghalaya were calculated and the peak rainfall time was noted. Then from the simulation, the time of flood arrival i.e., the time when discharge exceeded 2000 m^3/s (corresponding to danger flood level) was noted (Table 6). The time interval between these two was calculated as the lag time of flood arrival. For the year 2004, the rainfall peak occurred at 09:00, 22 June and the flood time from simulation was 19:00, 22 June. So, the lag time was 10 hours. Similarly, the lag time was evaluated for each study year and shown in table. It was observing that the lag time gradually decreased.

Year	Run	Time of Peak Rainfall in Meghalaya	Time of Flood	Lag time (hr)
2002	Simulation	15 June 21:00	16 June 09:00	12
2004	Calibration	22 June 09:00	22 June 19:00	10
2009	Validation	27 July 21:00	28 July 06:00	9
2011	Simulation	20 July 15:00	21 July 00:00	9
2017	Simulation	13 June 03:00	13 June 11:00	8
2022	Simulation	16 June 11:00	16 June 18:00	7

Table 6. Year wise lag time between rainfall and flood arrival

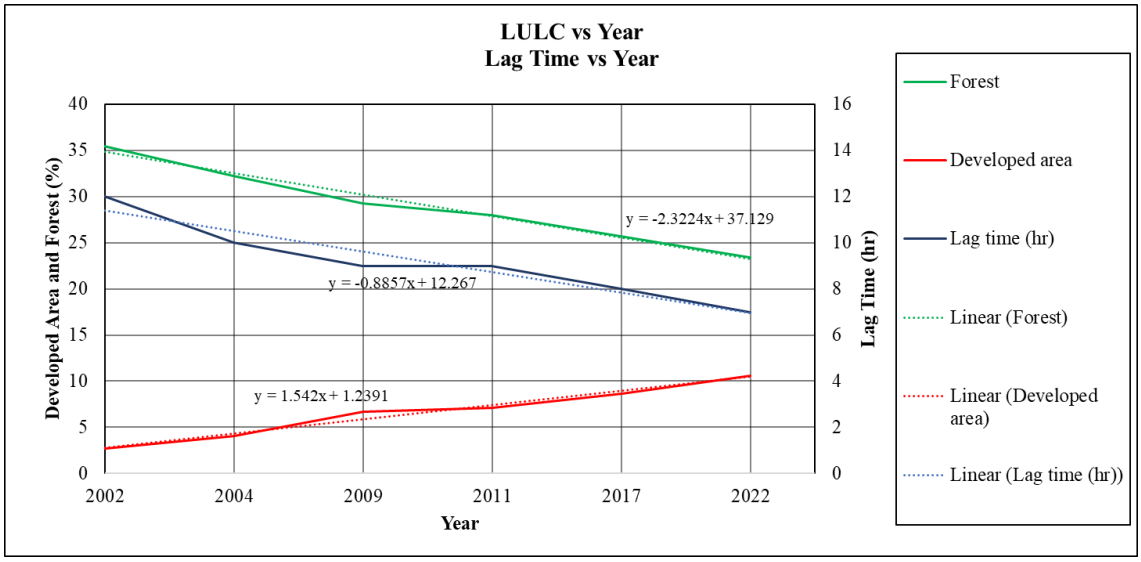

Figure 8. Relation between LULC and Lag time

The lag time of flood, forest area percentage and developed area percentage of each study year was plotted against time (Figure 8). The graph shows that as the forest area decreases and built-up area increases, the lag time also decreases due to increased imperviousness and runoff. This result is significant because it shows how the LULC changes has accelerated the arrival of runoff due to precipitation in Meghalaya to the Sylhet region, resulting in earlier flash floods than previous years. The lowest lag time was observed for 2022, when the flood arrived just 7 hours after the rainfall peak in Meghalaya.

4. CONCLUSION

Analysis of the Land Use/Land Cover (LULC) histogram plot reveals a discernible trend: a decline in canopy cover and a concurrent rise in developed areas within our study zone over the years. This shift contributes to a consistent escalation in impervious surfaces within the subbasin, evident in the percent imperviousness plot across the temporal spectrum. The continuous augmentation of imperviousness leads to accelerated runoff, resulting in a noticeable reduction in lag time between rainfall and the peak flood.

The perpetually increasing impervious surfaces prompt a swifter accumulation of runoff, diminishing the time interval between precipitation and the onset of peak flooding. In simpler terms, the flash flood occurrence is markedly earlier in recent years compared to previous periods. This temporal shift underscores the significant impact of urbanization on hydrological dynamics in the area. The diminishing lag time raises concerns about the region's vulnerability to flash floods and underscores the urgency of effective stormwater management strategies. Recognizing these trends in land use and their implications on runoff patterns is crucial for developing proactive measures to mitigate the escalating risks associated with rapid urban development in the study area.

ACKNOWLEDGEMENTS

We would like to express our heartiest gratitude to Mr. Ovi Ranjan Saha, Lecturer of Department of Water Resources Engineering, Bangladesh University of Engineering and Technology, for his helpful suggestion, comments and continuous support and encouragement throughout this research work.

REFERENCES

Adnan, M., & Bhuiyan, R. (2010). *Multi-Model Application for Climate Change Projections for Bangladesh and Assessment of Their Impacts on Small Drinking Water Systems*. *October*.

Alamgir, M., Khan, N., Shahid, S., Yaseen, Z. M., Dewan, A., Hassan, Q., & Rasheed, B. (2020). Evaluating severity–area–frequency (SAF) of seasonal droughts in Bangladesh under climate change scenarios. *Stochastic Environmental Research and Risk Assessment*, *34*(2), 447–464. https://doi.org/10.1007/s00477-020-01768-2

Arnold, J. G., Youssef, M. A., Yen, H., White, M. J., Sheshukov, A. Y., Sadeghi, A. M., Moriasi, D. N., Steiner, J. L., Amatya, D. M., Skaggs, R. W., Haney, E. B., Jeong, J., Arabi, M., & Gowda, P. H. (2015). Hydrological processes and model representation: Impact of soft data on calibration. *Transactions of the ASABE*, *58*(6), 1637–1660. https://doi.org/10.13031/trans.58.10726

Chen, A., Giese, M., & Chen, D. (2020). Flood impact on Mainland Southeast Asia between 1985 and 2018—The role of tropical cyclones. *Journal of Flood Risk Management*, *13*(2), 1–13. https://doi.org/10.1111/jfr3.12598

Das, M. K., M Saiful Islam, A. K., Jamal Uddin Khan, M., & Karmakar, S. (2017). Numerical Simulation of Flash-Flood-Producing Heavy Rainfall of 16 April 2016 in NE Regions of Bangladesh. *Vayu Mandal*, *43*(2), 2017.

Dietz, M. E. (2007). Low impact development practices: A review of current research and recommendations for future directions. *Water, Air, and Soil Pollution*, *186*, 351–363.

El Alfy, M. (2016). Assessing the impact of arid area urbanization on flash floods using GIS, remote sensing, and HEC-HMS rainfall-runoff modeling. *Hydrology Research*, *47*(6), 1142–1160. https://doi.org/10.2166/nh.2016.133

Feidas, H. (2010). Validation of satellite rainfall products over Greece. *Theoretical and Applied Climatology*, *99*(1–2), 193–216. https://doi.org/10.1007/s00704-009-0135-8

Ghannadi, M. A., Alebooye, S., Izadi, M., & Ghanadi, A. (2023). Vertical Accuracy Assessment of Copernicus Dem (Case Study: Tehran and Jam Cities). *ISPRS Annals of the Photogrammetry, Remote Sensing and Spatial Information Sciences*, *10*(4/W1-2022), 209–214. https://doi.org/10.5194/isprs-annals-X-4-W1-2022-209-2023

Islam, S. N. (2016). Deltaic floodplains development and wetland ecosystems management in the Ganges–Brahmaputra–Meghna Rivers Delta in Bangladesh. *Sustainable Water Resources Management*, *2*(3), 237–256. https://doi.org/10.1007/s40899-016-0047-6

Jain, S. K., Mani, P., Jain, S. K., Prakash, P., Singh, V. P., Tullos, D., Kumar, S., Agarwal, S. P., & Dimri, A. P. (2018). A Brief review of flood forecasting techniques and their applications. *International Journal of River Basin Management*, *16*(3), 329–344. https://doi.org/10.1080/15715124.2017.1411920

Janicka, E., & Kanclerz, J. (2023). Assessing the Effects of Urbanization on Water Flow and Flood Events Using the HEC-HMS Model in the Wirynka River Catchment, Poland. *Water (Switzerland)*, *15*(1). https://doi.org/10.3390/w15010086

Kementerian Kesehatan RI. (2018). *Profil Kesehatan Indonesia 2015*. *1227*(July), 496. https://doi.org/10.1002/qj

L., D., H., A., D., S.-T., & D., C. (2001). Flash Flood Forecasting with Coupled Precipitation Model in Mountainous Mediterranean Basin. *Journal of Hydrologic Engineering*, *6*(1), 1–10. https://doi.org/10.1061/(ASCE)1084-0699(2001)6:1(1)

Mandal, S. P., & Chakrabarty, A. (2016). Flash flood risk assessment for upper Teesta river basin: using the hydrological modeling system (HEC-HMS) software. *Modeling Earth Systems and Environment*, *2*(2), 1–10. https://doi.org/10.1007/s40808-016-0110-1

Nijhawan, R., Srivastava, I., & Shukla, P. (2017). Land cover classification using super-vised and unsupervised learning techniques. *2017 International Conference on Computational Intelligence in Data Science(ICCIDS)*, 1–6. https://doi.org/10.1109/ICCIDS.2017.8272630

P Fernandes, A. C., R Fonseca, A., Pacheco, F. A. L., & Sanches Fernandes, L. F. (2023). Water quality predictions through linear regression - A brute force algorithm approach. *MethodsX*, *10*, 102153. https://doi.org/https://doi.org/10.1016/j.mex.2023.102153

Qi, W., Ma, C., Xu, H., Chen, Z., Zhao, K., & Han, H. (2021). A review on applications of urban flood models in flood mitigation strategies. In *Natural Hazards* (Vol. 108, Issue 1). Springer Netherlands. https://doi.org/10.1007/s11069-021-04715-8

Rashid, B., Islam, S. U., & Islam, B. (2015). River morphology and evolution of the Barind Tract, Bangladesh. *Journal of Nepal Geological Society*, *49*(1), 65–76.

https://doi.org/10.3126/jngs.v49i1.23144

Rashid, M., & Yasmeen, R. (2018). Cold Injury and Flash Flood Damage in Boro Rice Cultivation in Bangladesh: A Review. *Bangladesh Rice Journal*, *21*(1), 13–25. https://doi.org/10.3329/brj.v21i1.37360

Saberi, A., Kabolizadeh, M., Rangzan, K., & Abrehdary, M. (2023). *Accuracy assessment and improvement of SRTM, ASTER, FABDEM, and MERIT DEMs by polynomial and optimization algorithm: A case study (Khuzestan Province, Iran)*. *15*(1). https://doi.org/doi:10.1515/geo-2022-0455

Severe, N. (1996). *Flash Flood Forecasting : An Ingredients-Based Methodology*. *December 96*, 560–581.

Shuvo, S. D., Rashid, T., Panda, S. K., Das, S., & Quadir, D. A. (2021). Forecasting of pre-monsoon flash flood events in the northeastern Bangladesh using coupled hydrometeorological NWP modelling system. *Meteorology and Atmospheric Physics*, *133*(6), 1603–1625. https://doi.org/10.1007/s00703-021-00831-z

Singh, R. K. (2018). *Lecture Notes in Civil Engineering Advances in Water Resources Engineering and Management*.

Vaze, J., Teng, J., & Spencer, G. (2010). Impact of DEM accuracy and resolution on topographic indices. *Environmental Modelling & Software*, *25*(10), 1086–1098. https://doi.org/https://doi.org/10.1016/j.envsoft.2010.03.014

WMO, & GWPS. (2003). Integrated Flood Management Case Study Bangladesh. *Report:*, 15.

Wu, J., Liu, H., Wei, G., Song, T., Zhang, C., & Zhou, H. (2019). Flash flood forecasting using support vector regression model in a small mountainous catchment. *Water (Switzerland)*, *11*(7). https://doi.org/10.3390/w11071327

Zanchetta, A. D. L., & Coulibaly, P. (2020). Recent Advances in Real-Time Pluvial Flash. *Water*, *12*.

U.S. Army Corps of Engineers. "HEC-HMS Technical Reference Manual (2023)